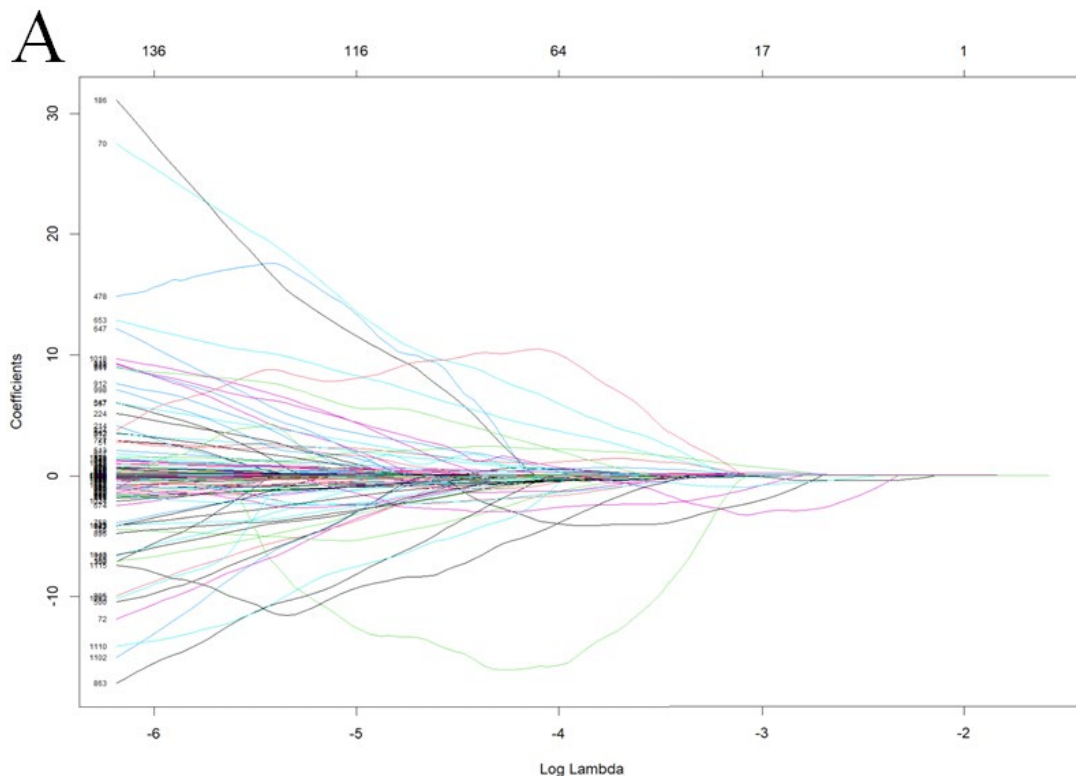
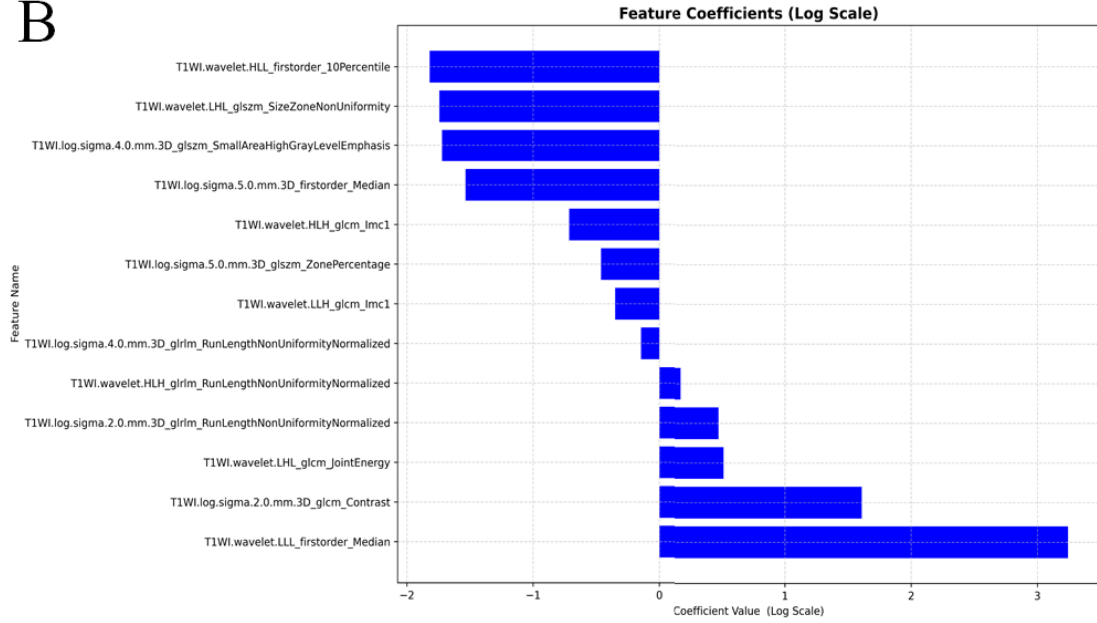
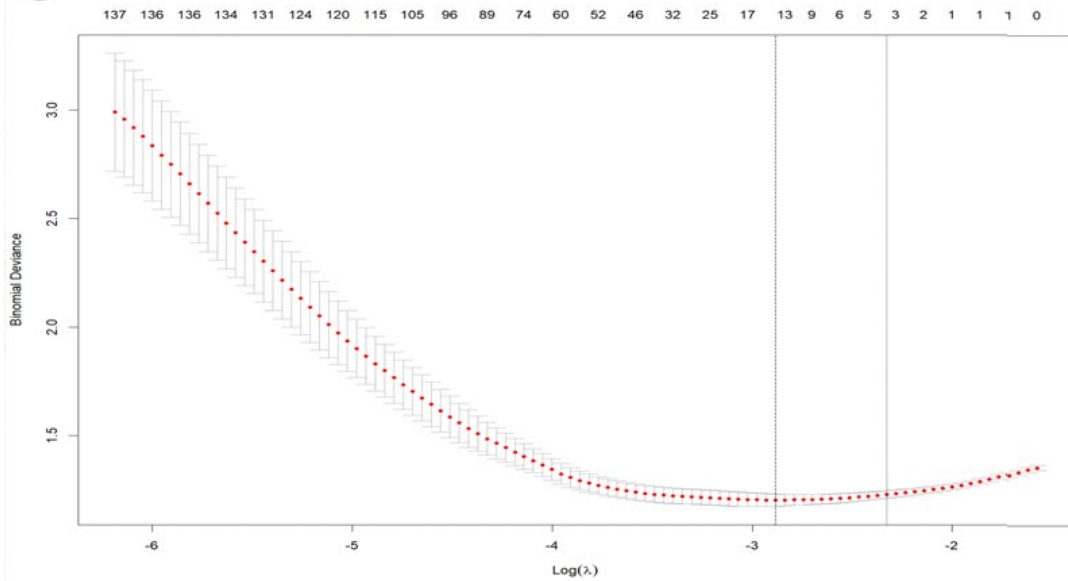


### Supplementary Figure 1

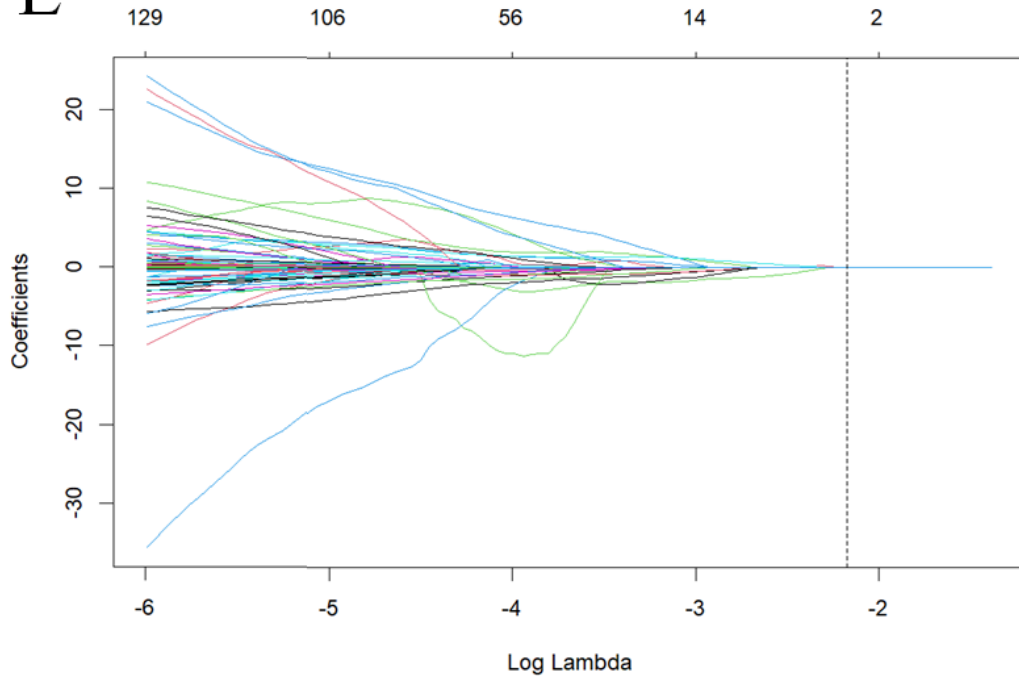
Radiomic features were extracted from T1WI, T2WI, and the combination of T1WI and T2WI imaging modalities for the lymph node. To predict lymph node metastasis (LNM), a radiomic signature score (radscore) was calculated using a final formula. For the selection of T1WI features (A-D) in predicting LNM, LASSO analysis was employed to identify the most valuable features. The analysis was conducted with a minimum Lambda value of 0.023 (C), resulting in obtaining the regression coefficients of LASSO (A). The final features and their corresponding coefficients were visualized in blue bars (B). The derived formula for calculating the T1WI radscore to predict LNM was obtained (D). Regarding T2WI features (E-H) in predicting LNM, LASSO analysis was carried out to determine the most valuable features. The analysis was performed with a minimum Lambda value of 0.023 (G), leading to obtaining the regression coefficients of LASSO (E). The final features and their corresponding coefficients were presented in blue bars (F). The derived formula for calculating the T2WI radscore to predict LNM was obtained (H). For the selection of combined T1WI and T2WI features (I-L) in predicting LNM, LASSO analysis was employed. The analysis was performed with a minimum Lambda value of 0.023 (K), resulting in obtaining the regression coefficients of LASSO (I). The final features and their corresponding coefficients were shown in blue bars (J). The final formula for calculating the T1WI&T2WI radscore to predict LNM was derived (L).



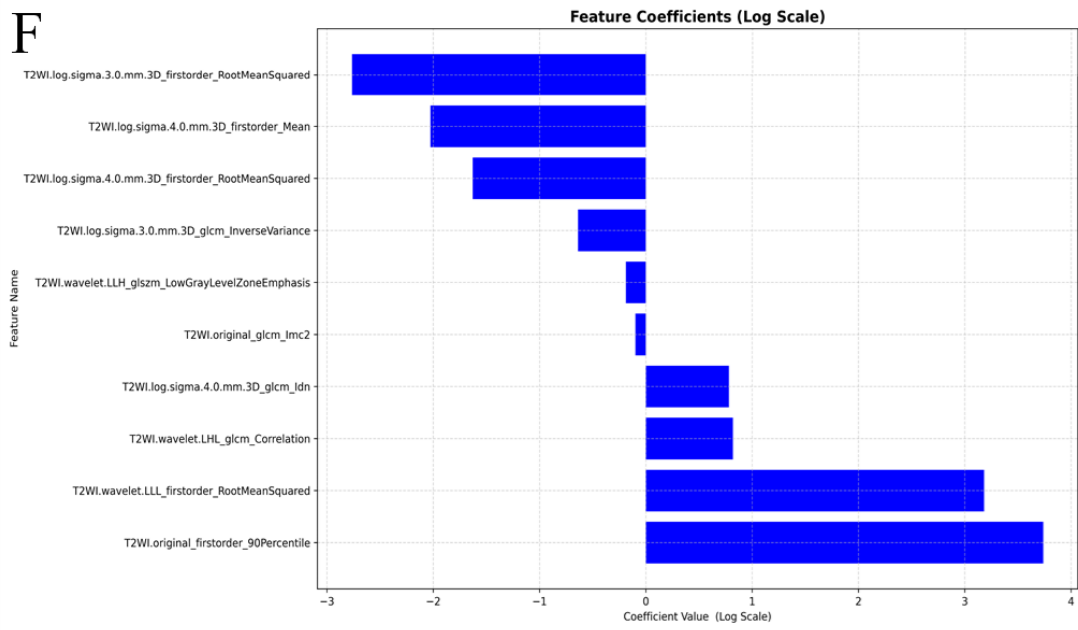
**B****C****D**

$$\begin{aligned}
 \text{T1WI-radscore} = & 0.445799134 * \text{T1WI.wavelet.LLH\_glcm\_Imc1} + \\
 & 0.192915264 * \text{T1WI.wavelet.HLH\_glcm\_Imc1} + \\
 & 0.018996554 * \text{T1WI.log.sigma.4.0.mm.3D\_glSZm\_SmallAreaHighGrayLevelEmphasis} + \\
 & 0.029204933 * \text{T1WI.log.sigma.5.0.mm.3D\_firstorder\_Median} + \\
 & 0.01512988 * \text{T1WI.wavelet.HLL\_firstorder\_10Percentile} + \\
 & 0.01808207 * \text{T1WI.wavelet.LHL\_glSZm\_SizeZoneNonUniformity} + \\
 & -0.024615575 * \text{T1WI.log.sigma.2.0.mm.3D\_glcm\_Contrast} + \\
 & -0.335969979 * \text{T1WI.log.sigma.2.0.mm.3D\_glrIm\_RunLengthNonUniformityNormalized} + \\
 & -1.396851111 * \text{T1WI.log.sigma.4.0.mm.3D\_glrIm\_RunLengthNonUniformityNormalized} + \\
 & -2.899637261 * \text{T1WI.log.sigma.5.0.mm.3D\_glSZm\_ZonePercentage} + \\
 & -0.307002868 * \text{T1WI.wavelet.LHL\_glcm\_JointEnergy} + \\
 & -0.672679438 * \text{T1WI.wavelet.HLH\_glrIm\_RunLengthNonUniformityNormalized} + \\
 & -0.000570756 * \text{T1WI.wavelet.LLL\_firstorder\_Median} + 1.0696351388
 \end{aligned}$$

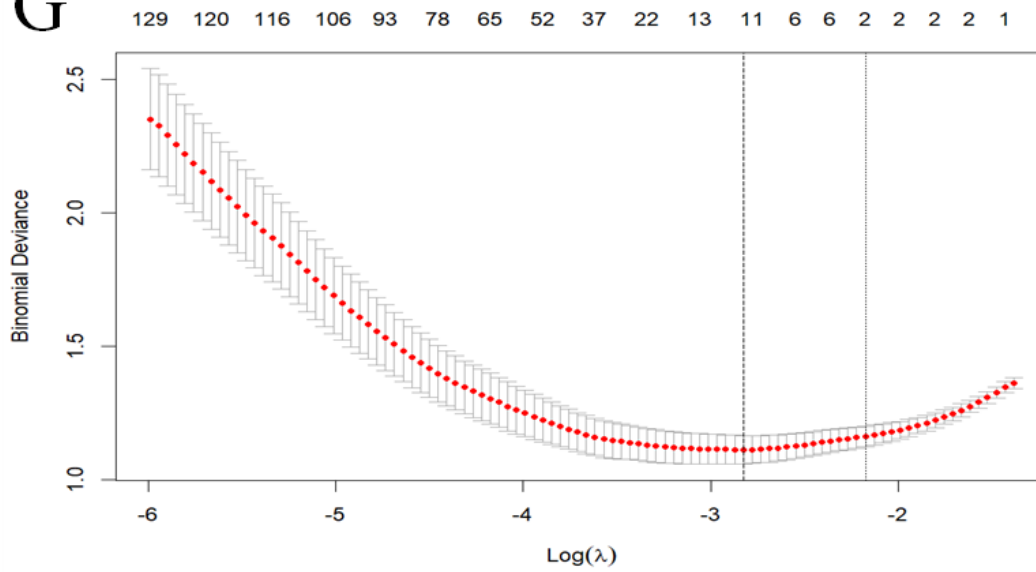
# E



# F



# G



# H

T2WI-radscore=  
-0.000183133\*T2WI.original\_firstorder\_90Percentile+  
-1.252403445\*T2WI.original\_glcmlmc2+  
0.001720382\*T2WI.log.sigma.3.0.mm.3D\_firstorder\_RootMeanSquared+  
0.230292662\*T2WI.log.sigma.3.0.mm.3D\_glcmlInverseVariance+  
0.009411352\*T2WI.log.sigma.4.0.mm.3D\_firstorder\_Mean+  
0.023526902\*T2WI.log.sigma.4.0.mm.3D\_firstorder\_RootMeanSquared+  
-0.165453207\*T2WI.log.sigma.4.0.mm.3D\_glcmlIdn+  
0.647880719\*T2WI.wavelet.LLH\_glszm\_LowGrayLevelZoneEmphasis+  
-0.151920182\*T2WI.wavelet.LHL\_glcmlCorrelation+  
-0.000657383\*T2WI.wavelet.LLL\_firstorder\_RootMeanSquared-  
7.5063443854